agronomy

MDPI

Article

Spectroscopic and Microscopic Analysis of Humic Acid Isolated from Stabilized Leachate HSs Fractionation

Zaber Ahmed [1,2], Mohd Suffian Yusoff [1,*], Nurul Hana Mokhtar Kamal [1], Hamidi Abdul Aziz [1] and Maria Roulia [3]

[1] School of Civil Engineering, Engineering Campus, Universiti Sains Malaysia, Nibong Tebal 14300, Penang, Malaysia
[2] Department of Civil Engineering, Model Institute of Science & Technology, DUET, Gazipur 1707, Bangladesh
[3] Inorganic Chemistry Laboratory, Department of Chemistry, National and Kapodistrian University of Athens, Panepistimiopolis, 157 71 Athens, Greece
* Correspondence: suffian@usm.my

Abstract: Refractory humic substances (HSs), which include humic and fulvic acid as well as hydrophilic portion, are the prime pollutants of stabilized landfill leachate with a concentrated color and chemical oxygen demand (COD). Spectroscopic and microscopic analysis of humic acid remaining in stabilized leachate as a pollutant contributor were conducted in this study. Microfiltration and centrifugation processes were applied to fractionate the humic acid from the HSs of stabilized leachate. The three-stage isolation process recovered a maximum of 1412 ± 2.5 mg/L (Pulau Burung leachate), 1510 ± 1.5 mg/L (Alor Pongsu leachate) at pH 1.5 and 1371 ± 2.5 mg/L (PBLS), and 1451 ± 1.5 mg/L (APLS) of humic acid (about 42% of the total COD concentration) at pH 2.5, which eventually indicates the efficiency of the process. The spectroscopic analysis of isolated humic acid through scanning electron microscopy (SEM), energy-dispersive X-ray (EDX), X-ray photoelectron spectroscopy (XPS), and Fourier transform infrared spectroscopy (FTIR) significantly indicates the existence of identical elements in the recovered humic acid. The subsequent reduction (around 37%, 36%, and 39%) in ultra-violet absorbance values (UV_{254}, UV_{280}), COD, and color in the humic acid isolated leachate indicates the acid's significant contribution as a toxic pollutant through aromaticity and conjugated double-bond compounds.

Keywords: stabilized leachate; humic substances; humic acid; microfiltration–centrifugation; spectroscopic analysis; XPS

Citation: Ahmed, Z.; Yusoff, M.S.; Mokhtar Kamal, N.H.; Abdul Aziz, H.; Roulia, M. Spectroscopic and Microscopic Analysis of Humic Acid Isolated from Stabilized Leachate HSs Fractionation. *Agronomy* **2023**, *13*, 1160. https://doi.org/10.3390/agronomy13041160

Academic Editor: Guangwei Ding

Received: 25 February 2023
Revised: 4 April 2023
Accepted: 10 April 2023
Published: 19 April 2023

1. Introduction

Rapid industrialization and economic development boost the upgradation of living standards, which eventually enhances the challenges of the generation and management of solid waste. Landfills are a privileged approach for rapidly increasing municipal solid waste (MSW) management due to simple operational mechanisms and cost-effectiveness [1]. A complex hydrological and biogeochemical interaction occurs during the progressive stabilization of solid waste after disposal at landfill sites, which eventually generates contaminated landfill leachate. This landfill leachate is a multifaceted fatal wastewater stream comprising massive amounts of recalcitrant and refractory HSs, heavy metals, and ammonia nitrogen [2]. Due to the existence of higher dissolved organics (humic substances with organic acids and macromolecular hydrocarbons), the biodegradability of stabilized leachate becomes less effective [3]. Humic acid is the dominating fraction (about 40–44%) of HSs in stabilized leachate, which is considered responsible for concentrated COD, a greenish-black color, and reduced biodegradability [4]. Therefore, the HSs of disposed leachate has an adverse health impact on human beings through water contamination [5]. The precise molecular structure of humic acid has not yet been explained [6]; however, various studies have reported that it comprises mainly the functional groups of unsaturated

conjugated double bonds such as aromatic rings and hydroxyl (-OH), carboxyl (-COOH), and carbonyl (-C=O) groups (Figure 1) [7]. Meanwhile, properly isolated humic acid may eradicate nitrogen, chlorinated solvents, heavy metals, and aqueous phosphorus efficiently through compound stabilization, which eventually can be implemented as the alleviator of soil by enhancing the accumulation potential [8]. The humic acid portion might enhance land fertility by releasing biologically active elements.

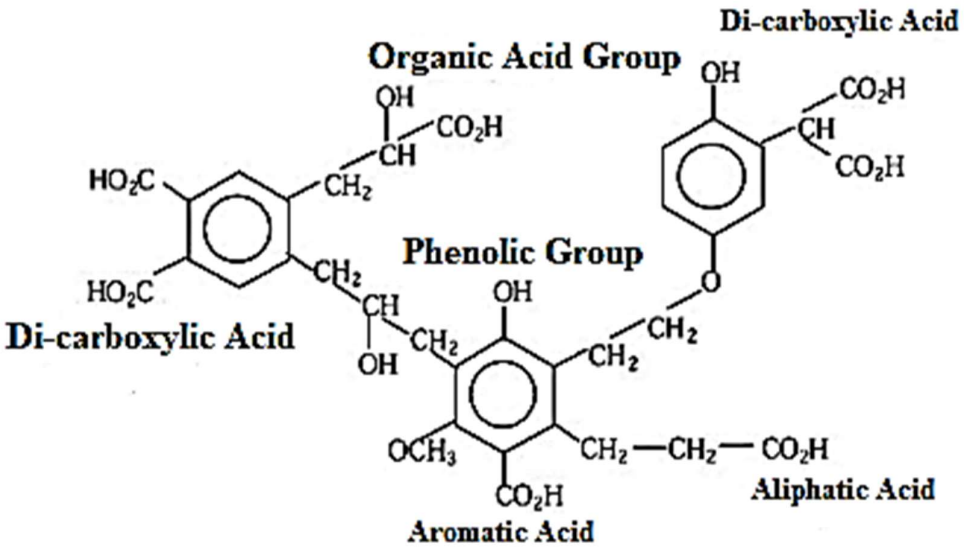

Figure 1. Typical humic acid structure.

Membrane filtration is a state-of-the-art physicochemical method for humic acid isolation from stabilized leachate [9]. Nanofiltration and reverse osmosis are efficient for eliminating dissolved organics from matured leachate, but they are expensive because of excessive energy consumption [10]. However, low-pressure ultrafiltration and microfiltration are cost-effective, while due to membrane fouling and flux reduction, they are inefficient [11].

The current study implemented a combination of microfiltration using hydrophilic PVDF (polyvinylidene fluoride) membrane filters and centrifugation for the isolation of humic acid from HSs fractions of stabilized leachate. Microfiltration was performed with an efficient flux, optimum surface area, and effective porosity. Hu et al. [12], Li et al. [13], and Gu et al. [14], along with other researchers, also recovered humic acid from stabilized leachate, but the precise spectroscopic and microscopic analysis of humic acid from HSs to identify as a pollutant contributor is the novel concern of this study. The main objectives of this study are to conduct a spectroscopic analysis of isolated humic acid through SEM-EDX, UV–Vis absorbance, XPS, and FTIR to trace the identical pollutants which contribute to stabilized leachate.

2. Materials and Methods

2.1. Collection of Stabilized Landfill Leachate

Stabilized leachate samples were collected from Pulau Burung landfill site (PBLS), Pulau Pinang and Alor Pongsu landfill site (APLS), Perak, confirming that there was no rain within three days before sampling. PBLS accumulates an average of 2000 tons of solid waste per day [15], while APLS currently receives around 200 metric tons of solid waste per day [16]. Air-tight polyethene containers (20 L) with a higher density and enfolded covers were utilized for collecting and preserving the leachate samples in a cold room (at 4 °C) [17]. Leachate samples were immediately transported to the laboratory (within 1 h) to preserve the originality and prevent any biological or chemical degradation before the experimental study [18].

2.2. Isolation of Humic Acid from HSs of Stabilized Leachate

Low-pressure microfiltration and centrifugation with a novel adjustment and increased precision were implemented to isolate humic acid from HSs through this study [19].

2.2.1. Microfiltration

The leachate samples of the PBLS and APLS were filtered through a hydrophilic polyvinylidene fluoride 0.45 µm white-colored membrane filter. Overall, 1 bar pressure was maintained at an optimum flux of 7 mL/min/cm^2 to mitigate the membrane fouling issue. Moreover, the membrane filters were washed consistently and carefully, applying 50 mL of distilled water until the UV_{254} of the effluent was almost equal to the ultra-pure water [20].

2.2.2. pH Adjustment

After optimum filtration, the pH value of the collected permeate was adjusted between 1.5 and 2.5 to optimize the recovery by applying 9 M of H_2SO_4 solution (Thermo Fisher Scientific, Waltham, MA, USA) and stirring gently for 15 min. Foaming and CO_2 generation were controlled through the slow addition of acid during pH adjustment. The samples were left for 18 h after pH adjustment to transform the dissolved humic acid into an insoluble form [21]. The application of this specific concentration confirmed a minimum (less than 1%) requirement of H_2SO_4 for pH adjustment, which eventually sustained the sample purity as well.

2.2.3. Centrifugation

Hettich Zentrifugen EBA 270 apparatus was employed to centrifuge the microfiltered and pH-adjusted leachate samples. A 25 to 50 min centrifuging period was applied at 3500 rpm to ensure the maximum humic acid recovery within the minimum amount of time. Figure 2 displays the schematic diagram of centrifugation.

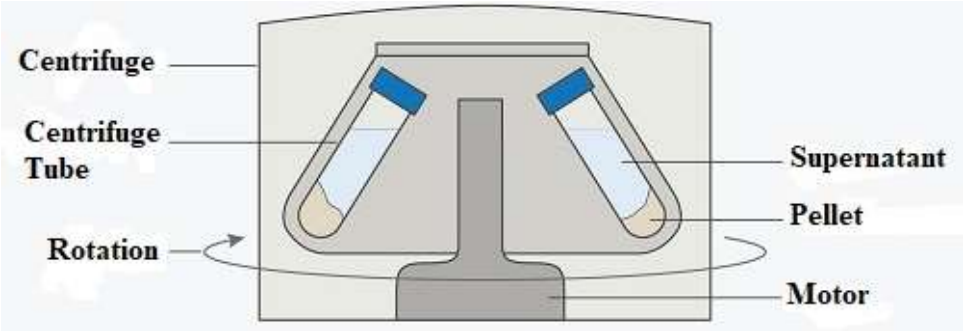

Figure 2. Schematic diagram of the centrifugation process.

The humic acid pellet was separated and filtered, applying a 1.5 µm filter paper. For quantifying humic acid, the filter paper mass (m_1) was deducted from the combined weight (m_2 = HA + filter paper).

Finally, the isolated humic acid was dried up at 45 °C for 12 h and pounded to prepare it in powdered form for characterization. Figure 3 displays the experimental procedure of humic acid isolation.

2.3. Microscopic Analysis of Isolated Humic Acid

SEM-EDX Analysis

The surface microstructure and energy-dispersive X-ray spectroscopy (EDX) were performed for humic acid using an FEI-Quanta 450 FEG scanning microscope. Energy-dispersive X-ray analyses were conducted under standard conditions. The samples were prepared accordingly in dried form. A small sample volume was retained on a static table with conductive carbon adhesive and was then enfolded to a flat level and dried up on a

hot surface. An ion sizzling device was applied for a 30-angstroms-thick platinum coating of the sample surface [22].

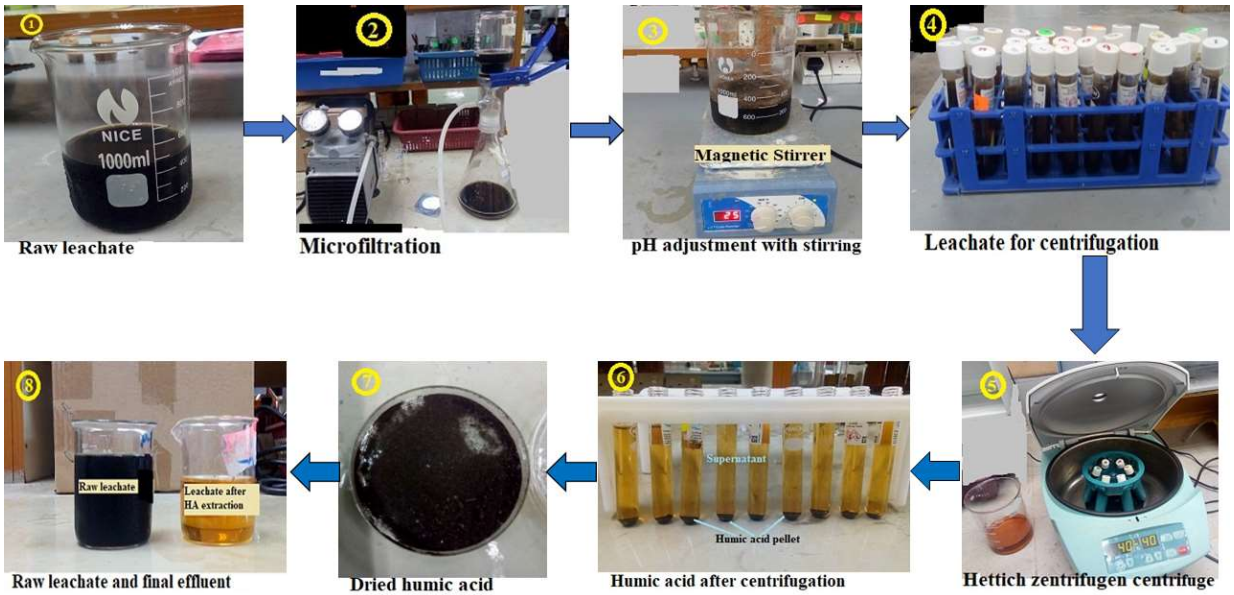

Figure 3. Humic acid isolation from stabilized leachate HSs fraction.

2.4. Spectroscopic Analysis of Isolated Humic Acid

2.4.1. UV–Vis Spectrum Analysis

The UV–Vis absorbance spectra of raw leachate samples and humic acid isolated leachate were recorded (wavelength 200–500 nm) on a Genesys 10S UV–Visible spectrophotometer (Thermo Fisher Scientific, 5229 Madison, WI, USA) using a 1 cm quartz cell. All the samples were diluted with ultra-pure water (UPW), the pH was adjusted from 6.0 to 7.0 before measuring, and Mile-Q water served as a reference solution. Absorbance values at 254 nm (E_2), 365 nm (E_3), and 280 nm (E_{280}) were determined according to Liu et al. (2015) to measure the E_2/E_3 ratios. Meanwhile, E_2/E_3 was reciprocally allied with the aromaticity and molecular weight, whereas they were directly proportional to the acidity, carboxyl group [-COOH] content, oxygen (O), and carbon (C) [20].

2.4.2. FTIR Spectroscopy

FTIR analyses for isolated humic acid from PBLS and APLS were conducted using an FTIR device, Spectrum IR Tracer-100 Series (Shimadzu, Tokyo, Japan). A homogeneous mixture of 1 mg of sample with 100 mg of KBr (pure spectrum) was prepared previously through thoroughly drying at 65 °C, grinding, and squeezing into a pellet appropriate for FTIR investigation. Subsequently, FTIR spectrometric analysis was performed within the spectra range of 4000 cm^{-1} and 400 cm^{-1}. Transmittance peaks were recognized according to already published articles related to the interpretation of the spectral peaks of FTIR, and the variance in the assimilated data was further understood by identifying patterns in the samples [23].

2.4.3. XPS Analysis

The XPS extensive and slender scan spectra were assimilated through the apparatus AXIS Ultra DLD, Kratos, UK. This device is equipped with an Al Kα X-ray source (1486.6 eV) at 10 mA and 15 kV. The analyzing area was 300 µm × 700 µm under 4.8E × 10^{-9} torr pressure. The ultra-vacuum atmosphere inside the sample analyses space used the multi-lane plate and delay line detector (DLD). The analyzer was operated in fixed analyzer transmission (FAT) mode with a pass energy of the semi-circular analyzer set at 160 eV for the survey

and broad scan. At the same time, 20 eV binding energy was set for the high-resolution scans or narrow scans, while the minimum magnification of scanning was ten times [24].

Commercially available CasaXPS software was used to examine the XPS data (version 2.3.16). After linear or Shirley-type background removal, the individual peaks were fitted using a Gaussian–Lorentzian function (SGL (50), CasaXPS) [25].

The spectra were analyzed using vision software, which included a visualization manager and processing mechanism. The background subtraction and curve fitting were carried out by the linear method. The binding energy was referenced to adventitious carbon at 284.6 eV.

2.5. Humic Acid Contribution as Pollutant (COD and Color)

The removal percentage of color, COD, or UV_{254} as the consequence of humic acid isolation was measured based on the values of the initial and final concentrations by applying Equation (1).

$$\% \text{ Removal} = \frac{C_{raw\ leachate} - C_{HA\ recovered\ leachate}}{C_{raw\ leachate}} \times 100 \quad (1)$$

where $C_{raw\ leachate}$ = raw leachate concentration of color, COD, and UV_{254}.

$C_{HA\ recovered\ leachate}$ = final effluent concentration of color, COD, and UV_{254}.

3. Results

3.1. Humic Acid Isolation

Before starting the humic acid isolation process, the collected leachate sample was simply characterized regarding its pH, dissolved oxygen, bio-chemical oxygen demand, color, and COD to identify the pollution level. The leachate sample was categorized as basic (maximum pH value 8.40 and 8.48, respectively), having concentrated a COD reading (average 3606 mg/L) which surpasses the 400 mg/L standard value (Environmental Quality Regulations 2009). Moreover, a very low (<0.1) BOD_5/COD ratio of these leachate samples indicates the higher existence of humic substances, a greater stability, and reduced biodegradability, with substantial contamination by refractory organic compounds [26]. The high concentration of SS (611 mg/L) and BOD_5 (average 281 mg/L), which is significantly higher in comparison with the standard (20 mg/L) (Environmental Quality Regulations 2009), specified the existence of higher organic contents in the sample as well. The dissolved organics are mostly responsible for the greenish-black color (5042 Pt-Co) of leachate.

The current study extracted a maximum of 1412 ± 2.5 mg/L (PBLS) and 1510 ± 2.5 mg/L (APLS) at pH 1.5 and 1371 ± 2.5 mg/L (PBLS) and 1451 ± 2.5 mg/L (APLS) of humic acid at pH 2.5, respectively (Figure 4). These humic acid portions are about 40% of the total COD concentration, which is consistent with Li et al. [13].

The humic acid isolation fluctuated due to the changes in the pH and centrifugation time, which remarkably influenced the removal of the blackish color and COD [17]. Humic acid separation was reduced when the pH was above 2.5, increasing at a lower pH (<2.5) value. The highest recovery was observed at pH 1.5, and it gradually decreased with the increase in the pH. The outcomes revealed that a lower pH or highly acidic environment is the most favorable for humic acid fractionation through converting it into an insoluble form. Meanwhile, the remaining fraction of HSs (fulvic acid and hydrophilic portion) can be isolated at a normal pH.

Besides the pH value, the centrifugation time also influences the isolation of humic acid significantly. The quantity of humic acid reached its maximum at 40 min. However, a 40 min centrifugation period confirmed 1380 ± 2.5 mg/L (PBLS) and 1462 ± 2.5 mg/L (APLS) of humic acid recovery at a pH value of 2.4 [27].

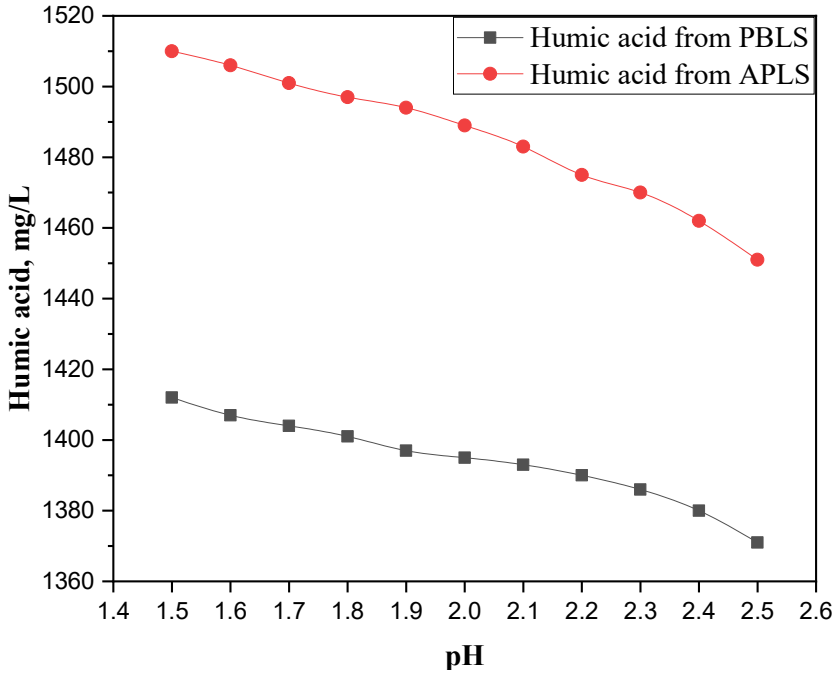

Figure 4. Humic acid isolation at varying pH levels.

3.2. Microscopic Characterization of Isolated Humic Acid

Surface Morphology and EDX Analysis Outcomes

Surface morphology was scrutinized as a part of this research study, employing scanning electron microscopy (SEM). Figure 5a,b display the SEM images of PBLS humic acid at 1 K and 4 K magnification, while Figure 5c depicts the EDX analysis outcome.

The humic acid flocs became even denser and larger, as displayed in Figure 5b, because of the molecular accumulation within the flocs. The image indicated the gathering of the widespread particles among the humic acid molecules, which specifies the occurrence of molecular accumulation. Figure 5c exhibits the existence of identical elements through the EDX outcomes. Carbon (50.74%) and oxygen (39.12%) are the significant elements in humic acid. The EDX results also show the marginal presence of sodium (Na), aluminum (Al), chlorine (Cl), and sulfur (S) components, which are well consistent with previous research on humic acid [8].

3.3. Spectroscopic Characterization of Isolated Humic Acid

3.3.1. FTIR Analysis Outcomes

FTIR spectroscopy is a well-recognized technique for providing particulars regarding specific molecular structures, molecular vibrations, and functional groups [21]. FTIR analyses were conducted in the current study to investigate the functional groups and bonding structure of extracted HA from PBLS (Figure 6a) and APLS (Figure 6b).

FTIR outcomes indicate the significant presence of aromatic compounds, carboxylic, and amide groups in the extracted humic acid. Broader peaks appearing at 2108.2 cm^{-1} (PBLS) and 2036.83 cm^{-1} (APLS) correspond to alkynes (C-C stretching), the C-O group (strong), and =C- H group (strong), while another peak at 1647 cm^{-1} and 1680 cm^{-1} represents the structural vibration of aromatic double bonds C=C [28]. A sharp peak at 1411 cm^{-1} and 1402.25 cm^{-1} is linked with the distortions of the carboxylic group or COO− irregular stretching, the existence of aromatic groups (C-C stretch, intense), and saturated hydrocarbons (C-H-C bend) [12]. Besides these, peaks also appear at 3170 cm^{-1} and 3128.54 cm^{-1}, which indicate the presence of C-H stretching in the carboxylic acid group (-COOH) along with H-bonded OH groups as well as 1°, 2° amines with trace N-H stretching [21]. Declining tendencies were detected for the peaks at 1647 cm^{-1}, 1680 cm^{-1} and 1411 cm^{-1}, and 1402.25 cm^{-1} in isolated humic acid (Table 1).

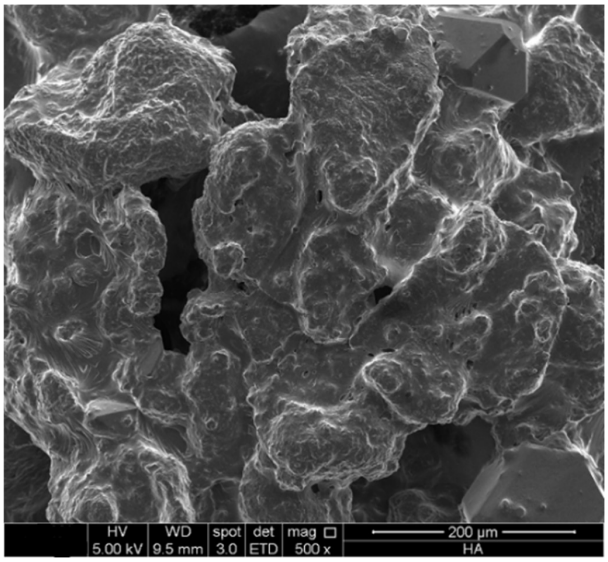

(**a**)

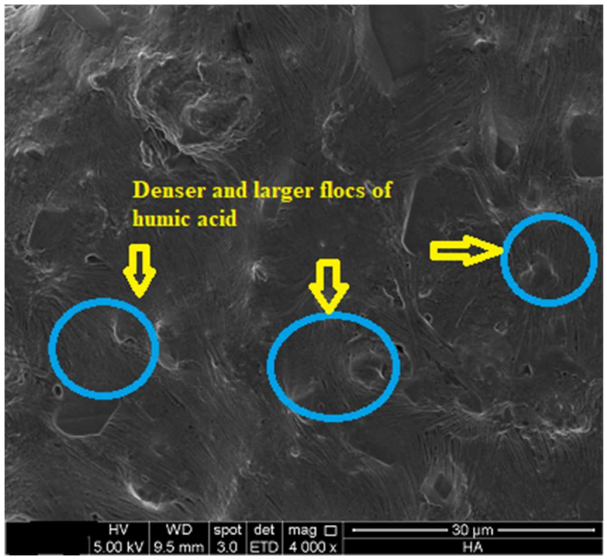

(**b**)

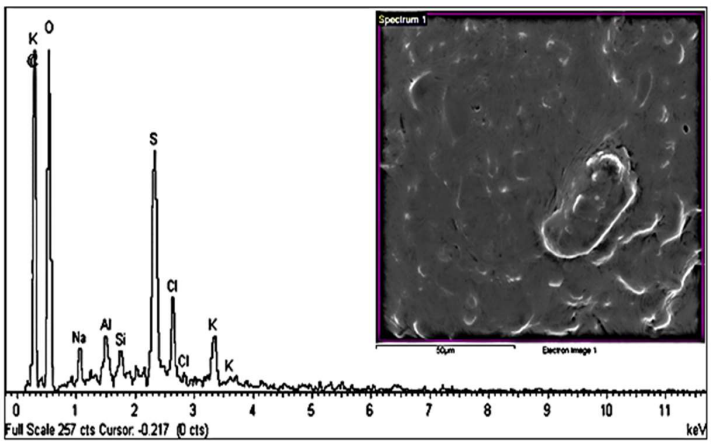

Elements	%Weight	%Atomic
C K	50.74	60.42
O K	39.12	34.97
Na K	1.1	0.69
Al K	0.63	0.34
Si K	0.45	0.23
S K	4.74	2.11
Cl K	1.85	0.75
K K	1.37	0.5
Totals	100	

(**c**)

Figure 5. SEM/EDX of isolated humic acid (**a**,**b**)—display the SEM images of PBLS humic acid at 1 K and 4 K magnification, (**c**)—depicts the EDX analysis outcome).

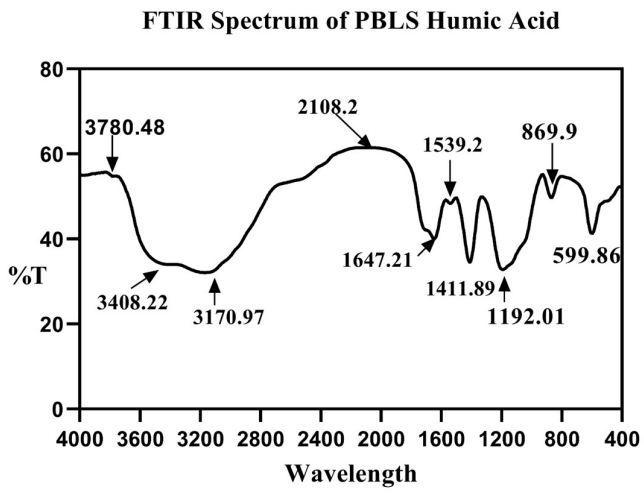

(**a**)

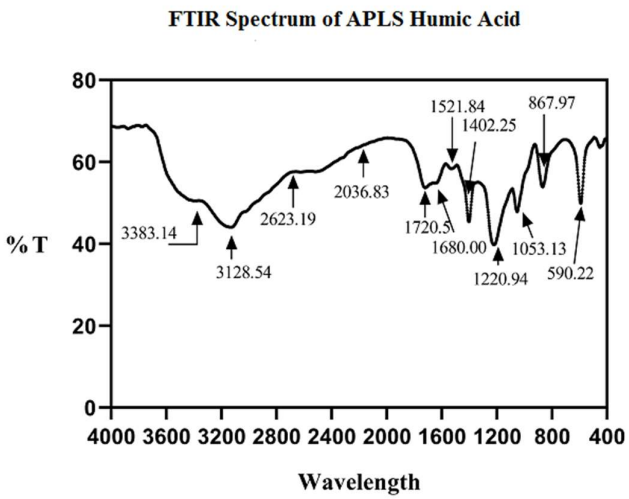

(**b**)

Figure 6. FTIR spectrum analyses of (**a**) PBSL humic acid and (**b**) APSL humic acid.

Table 1. Overview of FTIR outcomes for isolated humic acid.

Objects	Wavelength	Apparent Binding Status and Vibrational Assignment	Functional Groups
HA extracted from PBLS	3780.48 cm^{-1}	Hydrogen bonded with O-H or N-H vibration	Alcohols, phenols
	3408.22 cm^{-1}	N-H bend	Secondary amines
	3170.97 cm^{-1}	C-H stretching in -COOH	Carboxylic acids and 1°, 2° amines
	2623.19	O-H stretch (hydrogen-bonded, which can conceal other peaks within this region.)	Carboxylic acids groups (always cover the entire region with identically wide peaks)
	2108.2 cm^{-1}	C-C stretch	Alkynes
	1647.21 cm^{-1}	C-C=C and C=O stretch	Alkenes, ketones
	1539.2 cm^{-1}	N-H bending vibration, N=O stretch	2° Amide and nitro groups
	1411.89 cm^{-1}	O-H vibration, C-C stretch	Aromatics, carboxylic
	1192.01 cm^{-1}	C-O asymmetric vibration, C-H wag	Alcohols, phenol, esters, alkyl halides
	1053.13	C-O stretch/C-O-C stretch	Esters, ethers
	869.9 cm^{-1}	N-H stretch or C-H bending vibration, =C-H and $=CH_2$ bend	Aromatics, alkenes
	599.86 cm^{-1}	C-Br and C-I stretch	Alkyl halides
HA extracted from APLS	3770.84	Hydrogen bonded with O-H or N-H vibration	Alcohols, phenols
	3383.14	N-H bend	Secondary amines
	3128.54	C-H stretching in -COOH	Carboxylic acids and 1°, 2° amines
	2515.18	O-H stretch	-COOH
	1720.5	C=O stretch	Carboxylic acids groups
	1680	C=O stretch	Carbonyl group
	1639.49	C=O stretch	Ketonic groups
	1521.84	N=O stretch	Nitro groups
	1402.25	S=O stretch	Sulfate groups
	1220.94	C-O stretch/C-O-C stretch	Alcohols, esters, ethers
	867.97	=C-H and $=CH_2$ bend	Alkenes

3.3.2. UV–Vis Spectrum Analysis

Figure 7 demonstrates the UV–Visible spectra of raw and humic acid-recovered leachate, recorded from 200 to 500 nm. The intensity of the spectrum reduced significantly after the isolation of humic acid, while numerous aromatics and unsaturated organic compounds were degraded. The raw leachate spectrum showed more complexity with intensive peaks between 210 nm and 375 nm. This might affect by the double bond organics, especially the ketones C=O and aromatic C=C functional groups chromophores with other organics [21]. The spectrum of humic acid for both leachates exhibits a similar development throughout the process. The outcomes indicated the abundant existence of macromolecule organics and polycyclic aromatic compounds in raw leachate humic acid with closely tied double bonds. However, the intensity of humic acid peaks is reduced significantly due to the removal of double bonds. Table 2 displays a further investigation of the organic characteristics of both PBLS and APLS through UV_{254} (absorbance at 254 nm) and UV_{280} (absorbance at 280 nm). The absorbance values of UV_{254} and UV_{280} are indicators of the aromaticity and hydrophobicity of the molecules [19]. The values of UV_{254} (18.995 for PBLS and 20.97 for APLS) and UV_{280} (14.9 for PBLS and 20.165 for APLS) for raw leachate exhibit a strong hydrophobicity and aromaticity, which declined after humic acid isolation.

The E_2/E_3 value of the HA-extracted leachate of PBLS (4.96) and APLS (3.2) are higher than those of raw leachate (4.2 and 2.569) (Table 2). This value (E_2/E_3) is considered directly proportionate to the carbon, oxygen, and carboxyl (COOH) content, whereas it is inversely proportional to the aromaticity and molecular weight. A comparatively lower ($\leq$4) value of E_2/E_3 is characteristic of humic acid fraction, indicating a higher molecular weight, while a higher ratio ($\geq$5) is the indicator of a lower molecular weight and the increased existence of fulvic acid mainly [21].

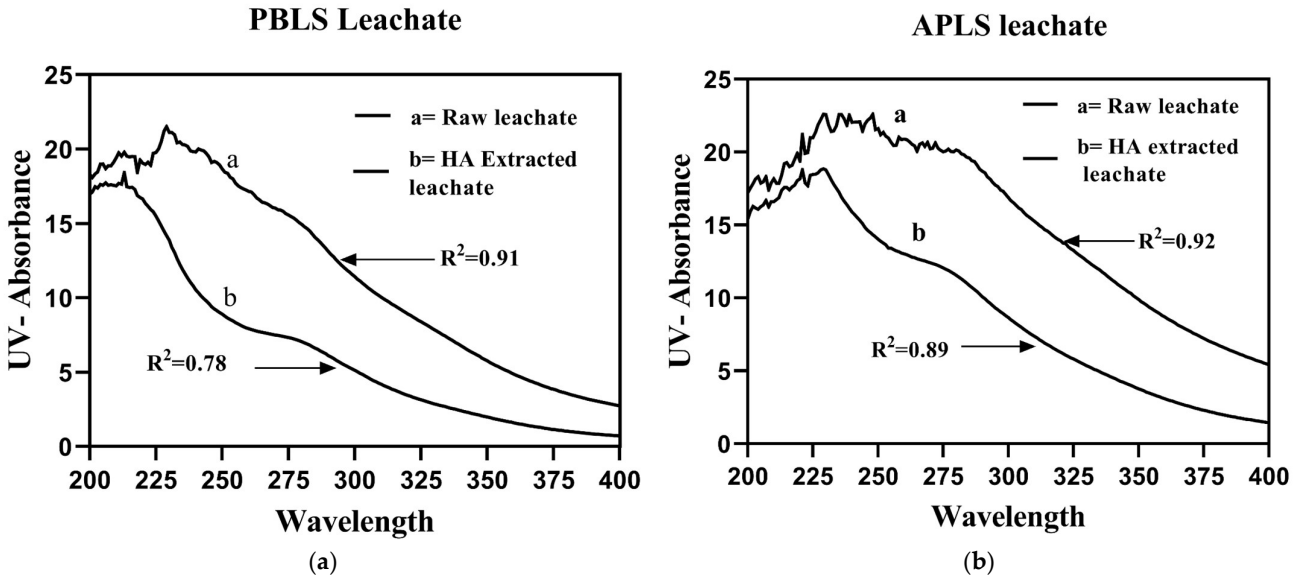

Figure 7. UV–Visible spectra for isolated humic acid (**a**) PBSL leachate and (**b**) APLS leachate.

Table 2. Outcomes of UV–Vis absorbance analysis.

UV-Absorbance	Raw Leachate	PBLS Humic-Acid-Extracted Leachate	% Removal	Raw Leachate	APLS Humic-Acid-Extracted Leachate	% Removal
UV254 (E_2)	18.995	11.975	37.01%	20.975	13.425	36.00%
UV280 (E_{280})	14.945	9.12	39.05%	20.165	11.57	42.62%
UV365 (E_3)	4.495	2.41	46.08%	8.16	4.19	48.6%
E_2/E_3	4.22	4.96	—	2.57	3.2	—

3.3.3. XPS Spectrum Analysis Outcomes

The surface elemental interaction of the isolated humic acid was further investigated using higher-resolution XPS. S2p, C1s, N1s, Na1s, Ag3d, and O1s were identified in the overall XPS spectra of humic acid samples. XPS is commonly used to investigate the variations in the surface configuration, elemental arrangement, and chemical condition. Figure 8 displays the XPS spectrum analysis outcomes of extracted humic acid from the PBLS leachate sample.

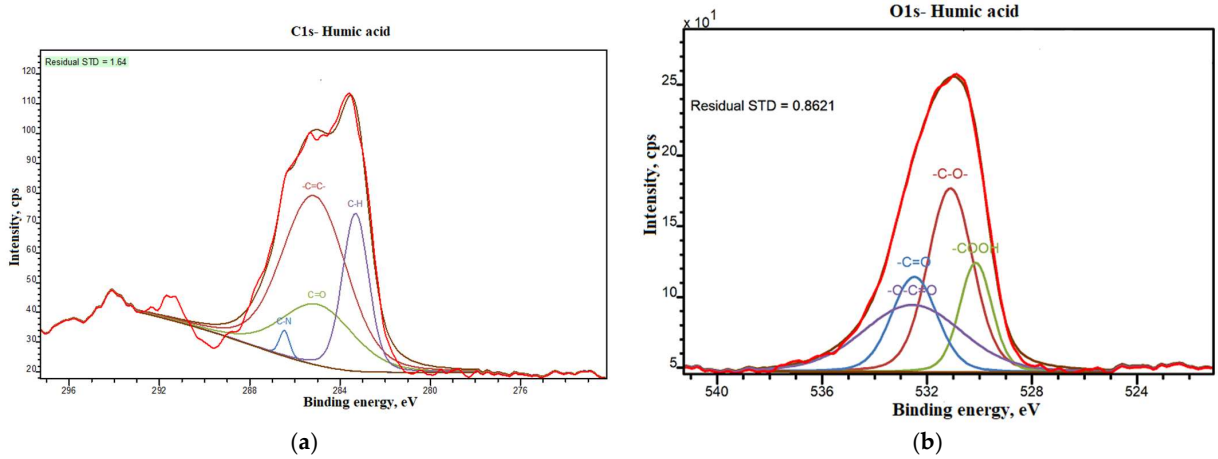

Figure 8. *Cont.*

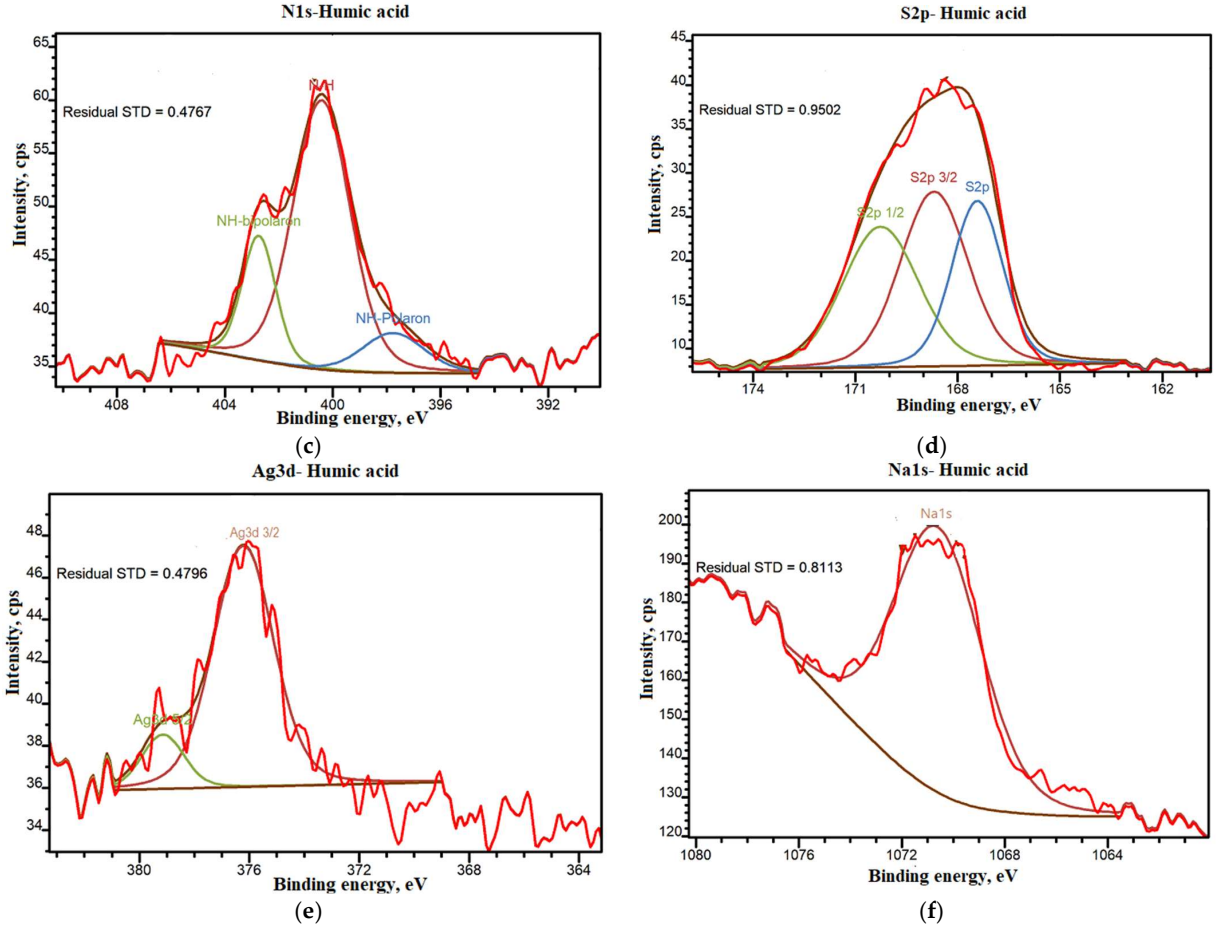

Figure 8. XPS analysis outcomes for humic acid (**a**) C1s; (**b**) O1s; (**c**) N1s; (**d**) S2p; (**e**) Ag3d and (**f**) Na1s.

Figure 8a shows the background-subtracted major focused level C1s spectra of recovered humic acid. Major C1s peaks were observed in extracted humic acid before coagulation at binding energies 289.35, 287.4, 286.6, 285.5, and 283.9 eV, which indicate the relevant carbon molecules [29]. Aromatic carbon (C=C), aliphatic carbon (C-H), carboxylic carbon (C=O), ether or alcohol carbon (C-O), and amide carbon (C-N) are the peaks that might be attributed to the identified binding energies [7]. The peak 286.6 is attributed to the π-π vibration of C-O (carboxylate group), referring to the particles bridging among the aromatic structure [30].

The high-resolution XPS analysis of extracted humic acid identified four major sorts of oxygen species in the O1s spectrum: C-O (531.37 eV), O-C=O (533.053 eV), C=O (532.21 eV), and -COOH (531.93 eV) corresponding to carbonyl, hydroxyl, and carboxylic groups (Figure 8b) [31].

Figure 8c displays the N1s spectrum from the XPS analysis of humic acid. Three main peaks were identified at binding energies of 398.5 eV, 400.4 eV, and 402.8 eV, respectively. These peaks can be attributed to primary or protonated amides, including a probable association with other structures such as amino acids. These outcomes correlate well with earlier research [32]. Protonated amino groups were observed in humic acid through XPS analysis gathered from the refractory portion of leachate. Surface complexation and electrostatic interaction among the humic acid molecules eventually promote this development [33].

The presence of a sulfate portion in humic acid as the oxidizing substance was identified by XPS analysis and shown in the higher sulfur resolution spectra of S2p at binding energies above 165 eV (Figure 8d). Complex multicomponent peaks containing numerous pairs of S2p 1/2–S2p 3/2 were found in the S2p spectra of humic acid. S2p spectra of extracted humic acid exhibited the incidence of sulfur couples, whose binding energy values

fluctuated between 164 eV and 173.8 eV and were found in diverse chemical states (central sulfur in the poly-sulfate terminal). Each component is made up of two S2p 3/2–S2p 1/2 doublets. All these findings are similar to earlier outcomes [34].

The XPS spectra of Ag3d of humic acid are displayed in Figure 9. The identical peaks of Ag 3d5/2 (379.16 eV) and Ag 3d3/2 (376.56 eV) from HA indicate the presence of a lower portion of silver-based salt [32]. The physicochemical situation inside the landfill, such as landfill age, types, waste composition, their atomic bonding, etc., [35] and the source of Ag ions are the influential factors of Ag3d binding energies. However, it is mentionable that the binding energies of Ag achieved from humic acid are a bit lower than other chemical substances ($AgNO_3$). Ag forms a coordination bond with the sulfur and nitrogen atoms, and electron pairs occupy the empty orbitals. Hence, this neutralizes a portion of the active charge and causes a reduction in the Ag3d binding energy.

A single intensive peak at 1071.69 eV (fwhm 1.4 eV) is traced in Na1s spectra during the XPS analysis of humic acid, which indicates a particular biochemical condition of the Na atom in humic acid (Figure 8f). The hexagonal form of the Na1s peak is no longer visible. The Na1s peak also indicates the existence of a minor portion through this analysis which is mostly ascribed to the impact of the atom's oxidation phase over the XPS characteristics [36]. Different numbers of spin–orbit pairs of the components with corresponding diverse binding energies were recognized in the isolated humic acid through XPS spectra after the curve-fitting procedure, which has been extensively authenticated by previous researchers [37].

3.4. Humic Acid Contribution as a Major Pollutant

The neutralization and protonation of negatively charged humic acid were developed in an acidic environment [38]. The maximum isolation of humic acid at optimum conditions (at pH 2.4 and 40 min centrifugation) obtained 36% and 39% COD and 39% and 44% color removal, which potentially unveiled the contribution of humic acid as pollutants (COD and color) of stabilized leachate.

However, significant variations in the humic acid isolated spectrum were observed (Figure 9), including the disappearance of several peaks, such as 2081 cm^{-1}, 1444 cm^{-1}, and 1340 cm^{-1}.

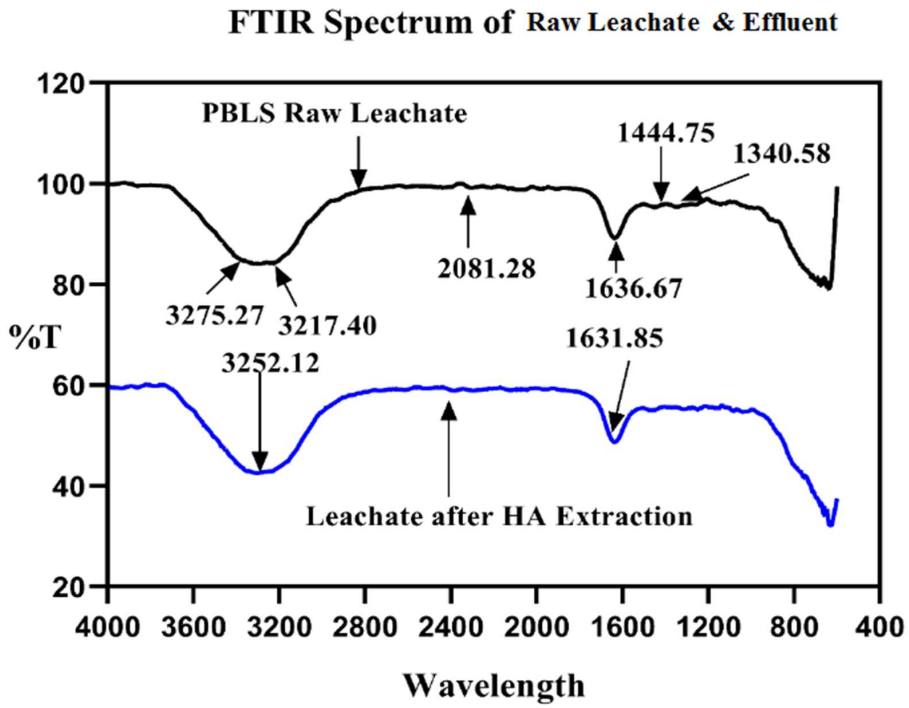

Figure 9. Differences between raw leachate and final effluent regarding humic acid isolation.

This affirms that a portion of aromatics, carboxylic, and amines were removed from raw leachate through humic acid separation. Meanwhile, the characteristic peaks at 1631 cm^{-1} and 3252 cm^{-1} appeared in humic-acid-extracted leachate (1631 cm^{-1}, 3252 cm^{-1}) with highly decreasing trends of intensities.

Table 3 exhibits the interrelationship of color and COD removal from matured leachate with humic acid recovery.

Table 3. Comparison of COD and color removal from leachate based on humic acid extraction.

	PBLS		APLS	
	Color (Pt-Co)	**COD (mg/L)**	**Color (Pt-Co)**	**COD (mg/L)**
Raw leachate	4139	3120	5367	3635
HA extracted leachate	2524.79	1996.8	3005.52	2206.44
% Removal	39%	36%	44.02%	39.30%

The nitrogen pair converts into positively charged particles under the acidic environment (lower pH), whereas the carboxyl group (–COOH) remains in bipolar form. Despite the fact that these functional groups in humic acid are treated as pollutants of leachate, they can also play a role in the betterment of agricultural soil as humus. Meanwhile, the alkaline environment (higher pH) reduces the bridging flocculation through increasing antipathy among the elemental particles [39].

4. Conclusions

The isolation of humic acid from stabilized leachate and its spectroscopic as well as microscopic analysis were studied. The study recovered a notable amount of humic acid from the HSs fraction of stabilized leachate sample as anticipated, which revealed the efficiency of the process eventually. Spectroscopic analysis confirms the presence of identical components and functional groups, which indicates the reusability of isolated humic acid for the improvement of soil properties. The outcomes also confirm that humic acid is free from other chemical substances, which may help agricultural soil eventually. Meanwhile, the microscopic analysis also displayed the proper size and shapes of the granules. Humic acid isolation promotes the significant removal of UV_{254} (37%), color (average 42%), and COD (average 38%), which eventually indicates a higher contribution.

Author Contributions: Conceptualization, Z.A.; methodology, Z.A..; software, Z.A. and M.S.Y.; validation, Z.A. and M.S.Y.; formal analysis, Z.A.; investigation, Z.A. and M.S.Y.; resources, M.S.Y.; data curation, Z.A.; writing—original draft preparation, Z.A.; writing—review and editing, M.S.Y., M.R. and N.H.M.K.; visualization, M.S.Y. and N.H.M.K.; supervision, M.S.Y., H.A.A. and N.H.M.K.; project administration, M.S.Y.; funding acquisition, M.S.Y. All authors have read and agreed to the published version of the manuscript.

Funding: This research was funded by Fundamental Research Grant Scheme (FRGS) of the Ministry of Higher Education, Malaysia, grant number 203/PAWAM/6071415.

Institutional Review Board Statement: Not applicable.

Informed Consent Statement: Not applicable.

Data Availability Statement: Research data supporting the reported results of this study will be made available upon contact with the corresponding author of this article.

Acknowledgments: The authors would like to convey their gratitude to the Solid Waste Management Cluster of the School of Civil Engineering, Universiti Sains Malaysia, for supporting the conduct of this study.

Conflicts of Interest: The authors declare no conflict of interest. The funders had no role in the design of the study; in the collection, analyses, or interpretation of the data; in the writing of the manuscript; or in the decision to publish the results.

References

1. Righetto, I.; Al-Juboori, R.A.; Kaljunen, J.U.; Mikola, A. Multipurpose treatment of landfill leachate using natural coagulants—Pretreatment for nutrient recovery and removal of heavy metals and micropollutants. *J. Environ. Chem. Eng.* **2021**, *9*, 105213. [CrossRef]
2. Chen, W.; Zhang, A.; Jiang, G.; Li, Q. Transformation and degradation mechanism of landfill leachates in a combined process of SAARB and ozonation. *Waste Manag.* **2019**, *85*, 283–294. [CrossRef] [PubMed]
3. Luo, H.; Zeng, Y.; Cheng, Y.; He, D.; Pan, X. Recent advances in municipal landfill leachate: A review focusing on its characteristics, treatment, and toxicity assessment. *Sci. Total. Environ.* **2019**, *703*, 135468. [CrossRef] [PubMed]
4. Liu, X.; Novak, J.T.; He, Z. Removal of landfill leachate ultraviolet quenching substances by electricity induced humic acid precipitation and electrooxidation in a membrane electrochemical reactor. *Sci. Total. Environ.* **2019**, *689*, 571–579. [CrossRef]
5. Song, Y.; Li, H.; Han, Y.; Lu, C.; Hou, Y.; Zhang, Y.; Guo, J. Landfill leachate as an additional substance in the Johannesburg-Sulfur autotrophic denitrification system in the treatment of municipal wastewater with low strength and low COD/TN ratio. *Bioresour. Technol.* **2019**, *295*, 122287. [CrossRef] [PubMed]
6. Segundo, I.D.B.; Gomes, A.I.; Souza-Chaves, B.M.; Park, M.; dos Santos, A.B.; Boaventura, R.A.; Moreira, F.C.; Silva, T.F.; Vilar, V.J. Incorporation of ozone-driven processes in a treatment line for a leachate from a hazardous industrial waste landfill: Impact on the bio-refractory character and dissolved organic matter distribution. *J. Environ. Chem. Eng.* **2021**, *9*, 105554. [CrossRef]
7. Jin, P.; Song, J.; Yang, L.; Jin, X.; Wang, X.C. Selective binding behavior of humic acid removal by aluminum coagulation. *Environ. Pollut.* **2018**, *233*, 290–298. [CrossRef]
8. Iskander, S.; Novak, J.T.; He, Z. Reduction of reagent requirements and sludge generation in Fenton's oxidation of landfill leachate by synergistically incorporating forward osmosis and humic acid recovery. *Water Res.* **2018**, *151*, 310–317. [CrossRef]
9. Wang, H.; Cheng, Z.; Sun, Z.; Zhu, N.; Yuan, H.; Lou, Z.; Chen, X. Molecular insight into variations of dissolved organic matters in leachates along China's largest A/O-MBR-NF process to improve the removal efficiency. *Chemosphere* **2019**, *243*, 125354. [CrossRef]
10. De Almeida, R.; Couto, J.M.D.S.; Gouvea, R.M.; Oroski, F.D.A.; Bila, D.M.; Quintaes, B.R.; Campos, J.C. Nanofiltration applied to the landfill leachate treatment and preliminary cost estimation. *Waste Manag. Res. J. Sustain. Circ. Econ.* **2020**, *38*, 1119–1128. [CrossRef]
11. Zielińska, M.; Kulikowska, D.; Stańczak, M. Adsorption—Membrane process for treatment of stabilized municipal landfill leachate. *Waste Manag.* **2020**, *114*, 174–182. [CrossRef] [PubMed]
12. Hu, L.; Liu, Y.; Zeng, G.; Chen, G.; Wan, J.; Zeng, Y.; Wang, L.; Wu, H.; Xu, P.; Zhang, C.; et al. Organic matters removal from landfill leachate by immobilized Phanerochaete chrysosporium loaded with graphitic carbon nitride under visible light irradiation. *Chemosphere* **2017**, *184*, 1071–1079. [CrossRef] [PubMed]
13. Li, Z.; Kechen, X.; Yongzhen, P. Composition characterization and transformation mechanism of refractory dissolved organic matter from an ANAMMOX reactor fed with mature landfill leachate. *Bioresour. Technol.* **2018**, *250*, 413–421. [CrossRef] [PubMed]
14. Gu, N.; Liu, J.; Ye, J.; Chang, N.; Li, Y.-Y. Bioenergy, ammonia and humic substances recovery from municipal solid waste leachate: A review and process integration. *Bioresour. Technol.* **2019**, *293*, 122159. [CrossRef]
15. Ahmed, Z.; Yusoff, M.S.; Kamal, N.H.M.; Aziz, H.A. Optimization of the humic acid separation and coagulation with natural starch by RSM for the removal of COD and colour from stabilized leachate. *Waste Manag. Res. J. Sustain. Circ. Econ.* **2021**, *39*, 1396–1405. [CrossRef]
16. Zakaria, S.N.F.; Aziz, H.A. Characteristic of leachate at Alor Pongsu Landfill Site, Perak, Malaysia: A comparative study. *IOP Conf. Ser. Earth Environ. Sci.* **2018**, *140*, 012013. [CrossRef]
17. Reis, B.G.; Silveira, A.L.; Teixeira, L.P.T.; Okuma, A.A.; Lange, L.C.; Amaral, M.C.S. Organic compounds removal and toxicity reduction of landfill leachate by commercial bakers' yeast and conventional bacteria based membrane bioreactor integrated with nanofiltration. *Waste Manag.* **2017**, *70*, 170–180. [CrossRef]
18. Yusoff, M.S.; Aziz, H.A.; Alazaiza, M.Y.D.; Rui, L.M. Potential use of oil palm trunk starch as coagulant and coagulant aid in semi-aerobic landfill leachate treatment. *Water Qual. Res. J.* **2019**, *54*, 203–219. [CrossRef]
19. Liu, Z.; Wu, W.; Shi, P.; Guo, J.; Cheng, J. Characterization of dissolved organic matter in landfill leachate during the combined treatment process of air stripping, Fenton, SBR and coagulation. *Waste Manag.* **2015**, *41*, 111–118. [CrossRef]
20. Dia, O.; Drogui, P.; Buelna, G.; Dubé, R.; Ihsen, B.S. Electrocoagulation of bio-filtrated landfill leachate: Fractionation of organic matter and influence of anode materials. *Chemosphere* **2017**, *168*, 1136–1141. [CrossRef]
21. Tahiri, A.; Richel, A.; Destain, J.; Druart, P.; Thonart, P.; Ongena, M. Comprehensive comparison of the chemical and structural characterization of landfill leachate and leonardite humic fractions. *Anal. Bioanal. Chem.* **2016**, *408*, 1917–1928. [CrossRef]
22. Liu, Z.; Li, X.; Rao, Z.; Hu, F. Treatment of landfill leachate biochemical effluent using the nano-Fe 3 O 4 /Na 2 S 2 O 8 system: Oxidation performance, wastewater spectral analysis, and activator characterization. *J. Environ. Manag.* **2018**, *208*, 159–168. [CrossRef]
23. Bolyard, S.C.; Reinhart, D.R.; Richardson, D. Conventional and fourier transform infrared characterization of waste and leachate during municipal solid waste stabilization. *Chemosphere* **2019**, *227*, 34–42. [CrossRef] [PubMed]
24. Liu, X.; Pang, H.; Liu, X.; Li, Q.; Zhang, N.; Mao, L.; Qiu, M.; Hu, B.; Yang, H.; Wang, X. Orderly Porous Covalent Organic Frameworks-based Materials: Superior Adsorbents for Pollutants Removal from Aqueous Solutions. *Innovation* **2021**, *2*, 100076. [CrossRef] [PubMed]

25. Cornette, P.; Zanna, S.; Seyeux, A.; Costa, D.; Marcus, P. The native oxide film on a model aluminium-copper alloy studied by XPS and ToF-SIMS. *Corros. Sci.* **2020**, *174*, 108837. [CrossRef]
26. Antony, J.; Niveditha, S.; Gandhimathi, R.; Ramesh, S.; Nidheesh, P. Stabilized landfill leachate treatment by zero valent aluminium-acid system combined with hydrogen peroxide and persulfate based advanced oxidation process. *Waste Manag.* **2020**, *106*, 1–11. [CrossRef] [PubMed]
27. Tejera, J.; Miranda, R.; Hermosilla, D.; Urra, I.; Negro, C. Treatment of a Mature Landfill Leachate: Comparison between Homogeneous and Heterogeneous Photo-Fenton with Different Pretreatments. *Water* **2019**, *11*, 1849. [CrossRef]
28. Ferraz, F.; Bruni, A.; Povinelli, J.; Vieira, E. Leachate/domestic wastewater aerobic co-treatment: A pilot-scale study using multivariate analysis. *J. Environ. Manag.* **2016**, *166*, 414–419. [CrossRef]
29. Yang, S.; Xu, Y.; Liu, C.; Huang, L.; Huang, Z.; Li, H. The anionic flotation of fluorite from barite using gelatinized starch as the depressant. *Colloids Surf. A Physicochem. Eng. Asp.* **2020**, *597*, 124794. [CrossRef]
30. Chen, H.; Li, Q.; Wang, M.; Ji, D.; Tan, W. XPS and two-dimensional FTIR correlation analysis on the binding characteristics of humic acid onto kaolinite surface. *Sci. Total. Environ.* **2020**, *724*, 138154. [CrossRef]
31. Shi, M.; Zhao, Z.; Song, Y.; Xu, M.; Li, J.; Yao, L. A novel heat-treated humic acid/MgAl-layered double hydroxide composite for efficient removal of cadmium: Fabrication, performance and mechanisms. *Appl. Clay Sci.* **2020**, *187*, 105482. [CrossRef]
32. Zhang, S.; Dang, J.; Lin, J.; Liu, M.; Zhang, M.; Chen, S. Selective enrichment and separation of Ag(I) from electronic waste leachate by chemically modified persimmon tannin. *J. Environ. Chem. Eng.* **2020**, *9*, 104994. [CrossRef]
33. Bhatnagar, A.; Sillanpää, M. Removal of natural organic matter (NOM) and its constituents from water by adsorption—A review. *Chemosphere* **2017**, *166*, 497–510. [CrossRef]
34. Fantauzzi, M.; Elsener, B.; Atzei, D.; Rigoldi, A.; Rossi, A. Exploiting XPS for the identification of sulfides and polysulfides. *RSC Adv.* **2015**, *5*, 75953–75963. [CrossRef]
35. Wdowczyk, A.; Szymańska-Pulikowska, A. Analysis of the possibility of conducting a comprehensive assessment of landfill leachate contamination using physicochemical indicators and toxicity test. *Ecotoxicol. Environ. Saf.* **2021**, *221*, 112434. [CrossRef]
36. Boumaiza, H.; Renard, A.; Robinson, M.R.; Kervern, G.; Vidal, L.; Ruby, C.; Bergaoui, L.; Coustel, R. A multi-technique approach for studying Na triclinic and hexagonal birnessites. *J. Solid State Chem.* **2019**, *272*, 234–243. [CrossRef]
37. Shi, Y.; Wells, G.; Morgenroth, E. Microbial activity balance in size fractionated suspended growth biomass from full-scale sidestream combined nitritation-anammox reactors. *Bioresour. Technol.* **2016**, *218*, 38–45. [CrossRef]
38. Roulia, M. Humic Substances: A Novel Eco-Friendly Fertilizer. *Agronomy* **2022**, *12*, 754. [CrossRef]
39. Roulia, M.; Vassiliadis, A.A. Water purification by potassium humate–C.I. Basic Blue 3 adsorption-based interactions. *Agronomy* **2021**, *11*, 1625. [CrossRef]